ELSEVIER

Applied Surface Science 111 (1997) 295–301

applied surface science

Submicrochannel plate multipliers

A.V. Raspereza [b,*], A.N. Govyadinov [a], A.S. Kurilin [b], V.N. Kukhnovetc [a], I.F. Emel'yanchik [b], G.A. Sidorenko [a], A.G. Volod'ko [c], C.A. Zakhvittcevich [a]

[a] *Institute of Electronics, Belarus Academy of Science, 22, Logojskii Trakt, Minsk 220841, Belarus*
[b] *National Center of Particle and High Energy Physics, 153, Bogdanovicha str., Minsk 220040, Belarus*
[c] *Joint Institute for Nuclear Research, Dubna 141980, Moscow region, Russia*

Received 1 July 1996; revised 23 August 1996; accepted 23 August 1996

Abstract

A theoretical investigation of alumina micron and submicron multichannel electron amplifiers was carried out. The theoretical study was based on multiplier performance Monte-Carlo simulation and general concepts of secondary electron emission theory. The simulation was performed for multipliers for which the length-to-diameter ratio was varied from 40 to 60 and the bias voltage from 600 to 1400 V. Calculations were made for the linear mode of multiplier operation under single electron stimulus. The simulation showed that alumina plates of the considered configurations are expected to possess a high gain (> 1000 at applied voltages exceeding 1.2 kV). The simulation also demonstrated that submicrochannel multipliers have faster response (< 30 ps), better temporal resolution (< 10 ps) and higher tolerance to strong axial (parallel with respect to channel axis) magnetic fields (up to ~ 4 T) than microchannel plates with the same length-to-diameter ratios. Anodic alumina submicrochannel plates with channel diameter 0.07–0.4 μm, length-to-diameter ratio up to 300 and an effective open area up to ~ 50% have been produced.

Keywords: Simulation; Microchannel plates; Anodic alumina; Submicrochannel plates

1. Introduction

Microchannel plates (MCP) are compact electron multipliers of high gain which are widely used in many pulse-counting applications requiring: (I) fast response; (II) good temporal resolution and (III) tolerance of strong magnetic fields [1–5]. Furthermore, such kind of devices were shown to possess high radiation resistance and high counting rate capability [6].

At present, MCP multipliers are considered as one of the possible alternatives to plastic scintillators, used in CMS hadron calorimeters [7], which are predicted to degrade at high radiation levels. But the prospect of using lead glass MCP in calorimetry seems very doubtful because of the high cost of such microchannel plates. Late in the 1960's, physicists from the USA [8] put forward the idea to make an MCP of anodic alumina (AA), emphasizing that Al_2O_3 also possesses high secondary electron yield. Alumina plates are expected to be much less expensive than those made of lead glass. Recently alumina MCP became available due to microchannel and submicrochannel anodic alumina structures etching technology developed at the Institute of Electronics,

* Corresponding author. Tel.: +7-172-314679; fax: +7-172-326075; e-mail: rasp@hep.belpak.minsk.by.

PII S0169-4332(96)00724-6

Belarus Academy of Science [9]. Therefore, our main interest was to investigate theoretically AA MCP and subMCP multipliers and compare them with standard lead glass MCP's.

2. Anodic alumina as substance for microchannel plates

Porous anodic alumina films are formed by electrochemical oxidation of aluminium in electrolytes containing agents slightly dissolving AA (such as weak acids, appropriate salts and their mixtures). AA typically consists of regular hexagonal arrays of uniform cells, which are parallel to each other and are created normal to the initial surface. Each individual cell has an axial pore. There is also a barrier layer of oxide between the aluminium anode and the bottom of the pores. The main geometrical characteristics of this model have been confirmed and elaborated by many authors [10–15]. The diameter of the cells is mainly determined by the voltage used in the aluminium anodization. It has been shown that the cell diameter is approximately equal to 2.75 nm/V for different electrolytes [10,14]. The pore diameter is determined by the nature of electrolyte, its temperature and concentration, current density and other features of the anodization process [12,13,16–19]. By varying the electrolyte and conditions of anodizing, the cell-to-pore ratio can be produced in the range from 1.71 up to 3.33 [10,20–22]. The pore size can be increased by selective etching of AA pore's walls [8,23]. A review of the AA morphology and modeling of its porous structure growth are presented in [23].

AA arrays are very suitable for creating submicrochannal plates. To produce an AA submicrochannel plate the barrier layer on the bottom of the pores has to be removed in order to finish the channel formation [8]. The AA makes it possible to form submicrochannel plates with channel diameter from 20 to 300 nm [23,24] and more (up to 0.7–0.8 μm [8]). The length-to-diameter ratio (L/D) can be varied in an extremely wide range and is limited by the minimal AA thickness due to mechanical stability and can be 10–500 at a 10 μm thickness. Using the AA local etching, the channel diameter can be produced in the range from 2 μm up to several mm [9]. Recent developments in micromachining based on AA [9], barrier layer removing methods [26] and the study of stable high temperature polycrystalline anodic alumina (PCAA) [25,27] open new prospects for producing submicrochannal plates based on anodic alumina.

So the AA makes it possible to create a wide range of micro- and submicrochannel plates. But until recently, as we know, the simulation of such plates has not been carried out.

3. Computer simulation

3.1. General description of the computer model

A number of attempts were made to describe the basic characteristics of MCP via Monte-Carlo simulation of a single plate operation under a single electron stimulus. In the present paper we followed the Monte-Carlo approach of Ito et al. [2], who used a model, consisting of two parallel plates with a spacing equal to the channel diameter. Contrary to these authors, we propose a cylindrical channel model, which seems more realistic in this case. Furthermore, we also consider the MCP tolerance to an axial magnetic field.

In the calculation of the electron trajectories and the multiplication factor the following assumptions were made:

(1) Wall charge and space charge saturation effects are ignored.

(2) The applied electric field is assumed parallel with the channel axis.

(3)The number of secondaries is determined by a Poisson distribution.

(4) The secondary electron yield is calculated according to the empirical formula [2,28]:

$$\delta = \delta_m \frac{4x}{(x+1)^2} \exp(-\alpha(1-\cos\gamma)),$$

where

$$x = \frac{E}{E_m}\sqrt{\cos\gamma},$$

E and γ are the collision energy and impact angle, respectively of electrons striking the channel wall;

δ_m is the maximum secondary electron yield, corresponding to electrons normally colliding with the emitting surface with energy E_m and α is a material constant. δ_m, E_m and α were chosen to be equal to:

(a) 4.0, 250 eV, 0.50 for lead glass (data, taken from Ref. [2]).

(b) 4.8, 350 eV, 0.50 for alumina (most 'optimistic' data, taken from Ref. [29]).

(5) Secondary electrons have a Maxwellian energy and cosine angular distribution. The mean value of the kinetic energy of the secondary electrons is assumed to be equal to 2 eV.

(6) At the first step of the simulation, primary electrons have an energy of 500 eV and strike the front surface of the plate at an angle of 10° with respect to the channel axis. Then these parameters are varied, in order to study the variation of MCP gain with the variation of energy and angle of incidence of primaries.

(7) The possibility for primaries to strike the dead interchannel region of front surface is not considered.

(8) Magnetic field influence on secondary electron emission is not taken into account.

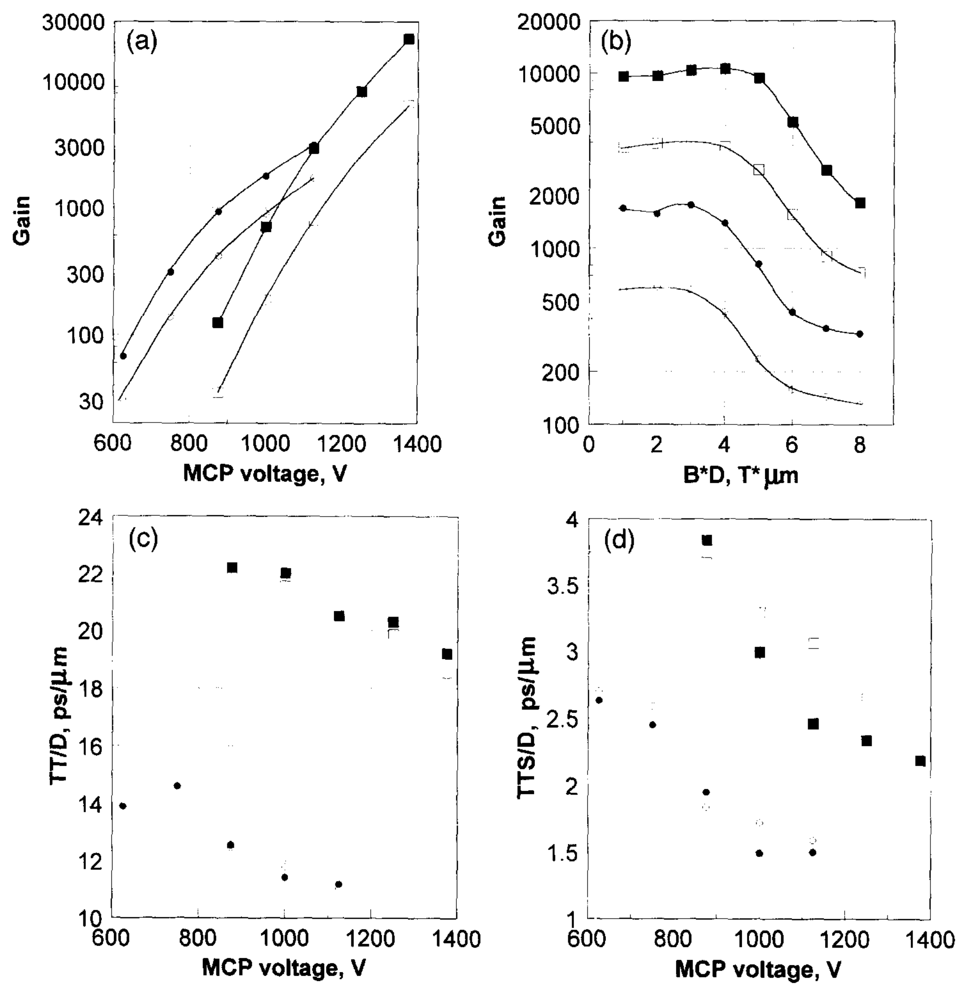

Fig. 1. Calculated characteristics of a single plate: gain versus voltage (a), axial magnetic field (b); transit time (c) and transit time spread (d) versus voltage for alumina (open symbols) and lead glass (solid symbols) plates, L/D 40, 60 (round and squared symbols respectively on plots (a), (c) and (d)), applied voltage 1000 and 1250 V (round and squared symbols, respectively, on plot (b) at L/D 50.

One should note that the present model, ignoring electron cloud space charge and channel wall surface charge influence on electron avalanche formation, possesses scaling symmetry. This means that at fixed applied voltage the pulse height distribution (PHD) depends on the length-to-diameter ratio (L/D) of the channels, while the transit time of the avalanche electrons increases linearly with increasing channel diameter (at fixed L/D). Furthermore, at fixed voltage and the L/D in the presence of magnetic field, PHD depends only on the product of magnetic field strength and channel diameter. These statements directly follow from the classical equation of charged particle motion in external electric and magnetic fields.

3.2. Computation

The calculations were performed on a SUN work station using FORTRAN language. The time re-

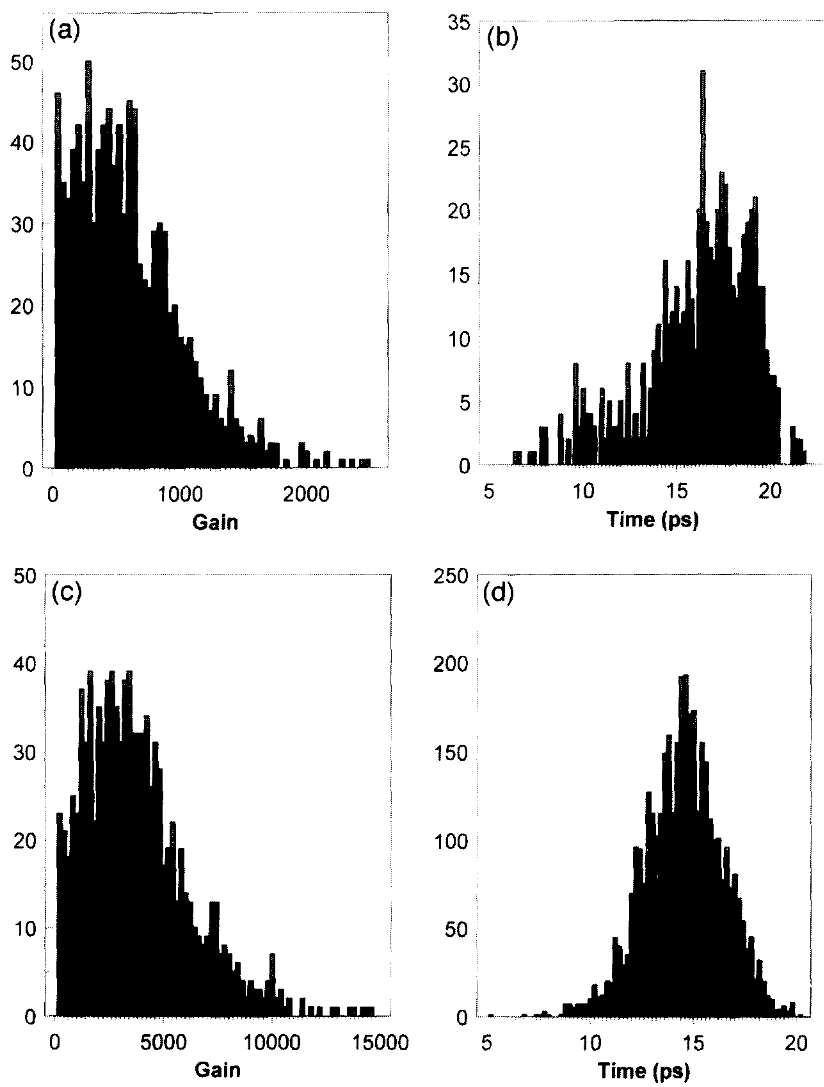

Fig. 2. Calculated pulse height distribution (a and c) and temporal response (b and d) of a single alumina plate. Histograms (a and b) correspond to applied voltage 1000 and (c and d) to 1250 V, respectively.

quired for sufficient statistic acquisition never exceeded 2 h.

3.3. Computer simulation results

Fig. 1a summarizes our calculations of gain versus voltage characteristics for standard lead glass (solid symbols) and alumina (open symbols) MCP with L/D at 40 (squared symbols) and 60 (round symbols). Calculations showed that at the same applied voltages the gain of alumina MCP is several times lower than that of a lead glass MCP.

The dependence of single-plate gain on axial magnetic field strength (at fixed applied voltages 1000 and 1250 V) is shown in Fig. 1b. The X-axis in this figure corresponds to the product of channel diameter and magnetic field strength. Axial magnetic field acts to decrease mean intercollision length of flight, thus decreasing collision energy of avalanche electrons, but increasing the number of electron collisions with the channel wall. At higher field strengths the former tendency dominates the latter and the MCP gain falls. Gain versus diameter-strength product plots indicate that the MCP of smaller diameters (submicrochannel plates) display better tolerance to an axial magnetic field.

Variations of the avalanche transit time (TT) and the transit time spread (TTS) with applied voltage are shown in Fig. 1c, d, respectively. The Y-axis in these figures stands for TT-to-diameter ratio and TTS-to-diameter ratio respectively. These plots indicate that for submicrochannel plates L/D is 40–60, the TT will be less than several tens of ps, while the TTS is less than several ps. This is why a MCP of smaller diameter (submicrochannel plates) should be used in pulse counting applications, requiring ultrafast response and good temporal resolution.

Fig. 2 shows typical PHD and temporal response of an alumina single plate with $L/D = 50$ to electrons with an energy of 500 eV, incident on the front surface at an angle of 10° with respect to channel axis. The great number of zero-entries in histograms Fig. 2a, c is explained by non-zero probability of losing signal in the first and subsequent stages of multiplication process. However, this probability sufficiently decreases with increasing MCP voltage. One can obtain the PHD of a single plate in the case of arbitrary transparency (effective open area) of a

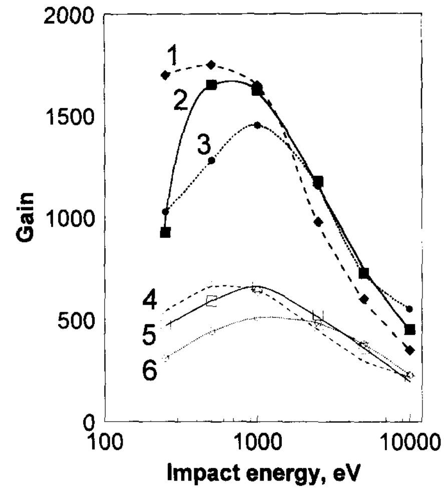

Fig. 3. Dependency of gain on impact energy of primaries: applied voltage 1000 V. Open and solid symbols stand for alumina and lead glass plates respectively. Angle of incidence takes values 5° (diamonds), 10° (circles) and 20° (squares).

plate by introducing a weight equal to the MCP transparency for every histogram bin except the bin corresponding to zero gain. The content of the latter must be increased by the number of 'lost' entries (lost primary electrons), striking the dead interchannel zone of the front surface of the MCP.

Fig. 3 demonstrates the variation of gain with the energy of the primary electrons initializing avalanche in MCP channels. Calculations showed that MCP electron multipliers are sensitive only to low energy (10^2–10^4 eV) electrons. This can be explained by the fact that electrons with higher energies deeply penetrate the emitting substance without exciting secondaries into the channel.

4. Fabrication of AA MCP

Submicrochannel plates with channel diameter 0.07...0.4 μm, L/D from 10 to 300 and effective open area up to ~50% have been designed. A typical AA plate micrograph is shown in Fig. 4.

Preliminary results on testing AA MCP showed that the leakage current of AA MCP is 5–6 orders of magnitude less than for standard lead glass MCP at the same applied voltages. Low gain, observed in

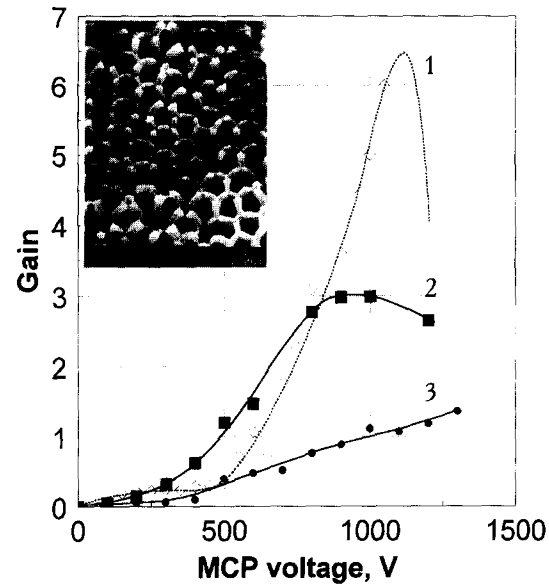

Fig. 4. Experimentally obtained gain versus voltage characteristics; (1) typical lead glass plate (channel diameter 10 μm, L/D 50 and transparency 58%), (2) anodic alumina plate (channel diameter 0.2 μm, L/D 200 and transparency 16%) and (3) anodic alumina plate (channel diameter 0.2 μm, L/D 300 and transparency 50%). (Typical AA plate micrograph is in the upper left corner of plot).

test experiments, is explained by suppression of avalanche caused by induced wall surface charge. In order to eliminate this effect it is necessary to increase the electrical conductivity of AA. Tentatively however, our experimental results demonstrate fundamental realizability of submicrochannel plates.

5. Conclusions

Computer simulation showed that alumina MCP of the considered configurations (L/D) are expected to possess:

(1) High gain (> 1000 for a single plate at a MCP voltage exceeding 1.2 kV). At the same applied voltages lead glass plates have a gain which is several times higher than that of alumina MCP's.

(2) Fast response (< 30 D (μm) ps) and good temporal resolution (< 10 D (μm) ps).

(3) Tolerance to the strong axial magnetic field (up to $4/D$ (μm) T) for applied voltage exceeding 1200 V.

One can conclude that MCP's of smaller diameters (submicrochannel plates) are preferable in applications requiring fast response, good temporal resolution and tolerance to strong axial magnetic fields.

Comparison of standard MCP's and AA subMCP's shows that it is possible to realize operating MCP's with submicron channels.

Thus the prospect of using alumina microchannel and submicrochannel plates in pulse-counting devices looks very promising for modern physics and electronic engineering.

References

[1] G.W. Fraser, Nucl. Instrum. Methods A 291 (1990) 559.
[2] M. Ito, H. Kume and K. Oba, Nucl. Sci. NS 31 (1984) 408.
[3] E.H. Eberhardt, IEEE Trans. Nucl. Sci. NS 28 (1981) 712.
[4] J.E. Bateman, R.J. Apsimon and F.E. Barlow, Nucl. Instrum. Methods 137 (1976) 61.
[5] K. Oba, M. Sugiyama, Y. Suzuki and Y. Yoshimura, IEEE Trans. Nucl. Sci. NS 26 (1979) 346.
[6] A.A. Derevshchikov, V.Yu. Khodyrev, V.I. Kryshkin V.E. Rakhmatov and A.I. Ronzhin, Preprint IHEP (Protvino, 1990) p. 90.
[7] Technical proposal: The compact muon solenoid, CERN/LHCC 94-38 (1994) 73.
[8] U.S. Patent No. 3626233.
[9] A.N. Govyadinov, I.L. Grigorishin and P.P. Mardilovich, ITG-Fachbericht, Vol. 132 (VDE, Verlag, 1995) p. 161.
[10] J.P. O'Sullivan and G.C. Wood, Proc. R. Soc. London Ser. A 317 (1970) 511.
[11] G.E. Thompson and G.C.Wood, in: Corrosion: Aqueous Processes and Passive Films, ed. J.C. Scully (Academic Press, London, 1983) p. 205.
[12] K. Ebihara, H. Takahashi and M. Magaymna, J. Met. Soc. Jpn. 33 (1982) 15.
[13] K. Ebihara, H. Takahashi and M. Magayama, J. Met. Soc. Jpn. 34 (1983) 548.
[14] V.P. Parkhutik and V.I. Shershulsky, J. Phys. D 25 (1992) 1258.
[15] K. Shimizu, K. Kobayashi, G.E. Thompson and G.C.Wood, Philos. Mag. A 66 (1992) 643.
[16] M. Nagayama, K. Yamura and H. Takahashi, Corros. Sci. 10 (1970) 617.
[17] N. Nagayama and K.Tamura, Electrochem. Acta 12 (1967) 1097.
[18] Y. Fukuda, Trans. Natl. Res. Inst. Met. 18 (1976) 197.
[19] D. Honicke, Aluminium (Dusseldorf) 65 (1989) 1154.
[20] T. Pavlovic and A. Ignatiev, Thin Solid Films 138 (1986) 97.
[21] V.A. Sokol, Dokl. Akad. Nauk. SSSR 30 (1986) 243. (In Russian)
[22] G.E. Thompson and G.C. Wood, Nature 290 (1981) 230.

[23] J. Randon, P.P. Mardilovich, A.N. Govyadinov and R. Paterson, J. Colloid Interface Sci. 169 (1995) 335.
[24] Watman International Limited, customer literature.
[25] P.P. Mardilovich, A.N. Govyadinov, N.I. Mukhurov, A.M. Rzhevskii and R. Paterson, J. Membrane Sci. 98 (1994) 131.
[26] International Patent Application, No. PCT/GB95/01646, Filled 11 July, 1995.
[27] P.P. Mardilovich, A.N. Govyadinov, N.I. Mazurenko and R. Paterson, J. Membrane Sci. 98 (1994) 143.
[28] A.M. Yakobson, Radiotekh. Elektron. 11 (1966) 1813. (In Russian)
[29] H. Bruining, Physics and Applications of Secondary Electron Emission (London, Pergamon Press, 1954).